Supplemental Information

Proteomic and Lipidomic Analysis of Nanoparticle Corona upon Contact with Lung Surfactant Reveals Differences in Protein, but not Lipid Composition

*Simon Sebastian Raesch[†,‡], Stefan Tenzer[§], Wiebke Storck[§], Alexander Rurainski[⊥], Dominik Selzer[⊥], Christian Arnold Ruge[†], Jesus Perez-Gil[‖], Ulrich Friedrich Schaefer[†], and Claus-Michael Lehr[†,‡]**

[†]Department of Pharmacy, Saarland University, 66123 Saarbruecken, Germany

[‡]HIPS - Helmholtz Institute for Pharmaceutical Research Saarland, Helmholtz Centre for Infection Research, 66123 Saarbruecken, Germany

[§]Institute of Immunology, Mainz University, 55131 Mainz, Germany

[⊥]Scientific Consilience GmbH, Saarland University, 66123 Saarbruecken, Germany

[‖]Department of Biochemistry and Molecular Biology, Faculty of Biology, Complutense University, 28040 Madrid, Spain

*corresponding author: claus-michael.lehr@helmholtz-hzi.de

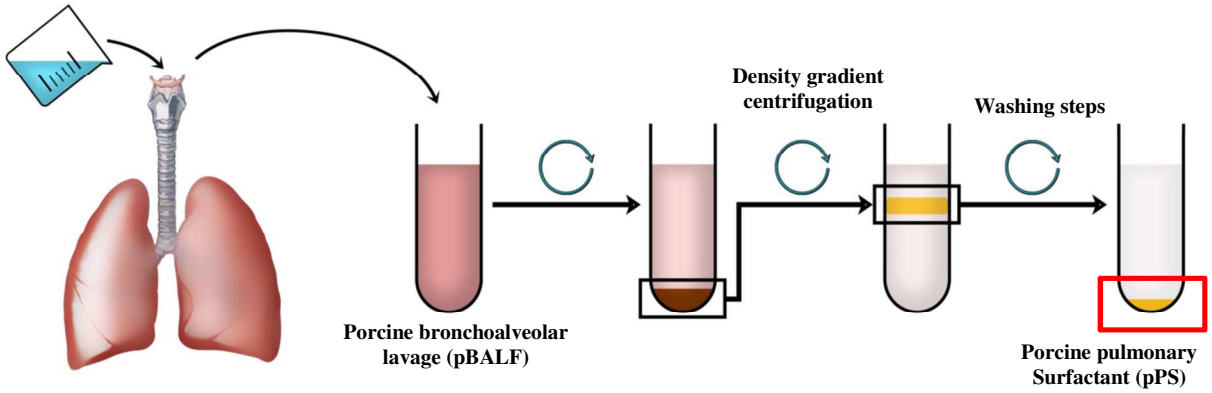

Figure S1: Schematic diagram of pPS isolation orginating from porcine lungs. Lungs from freshly slaughtered pigs were chosen in the slaughterhouse by their apparent intact, non-damaged appearance and lavaged immediately with physiological sodium chloride solution under application of massage. Clear pBALF was centrifuged at low speed for cell debris removal and frozen until further purification. Thawed pBALF was centrifuged and the supernatant was discarded. The accumulated pellets were dispersed in a sodium bromide solution. Native surfactactant vesicles with a density higher than 1.10 g/ml were separated by density centrifugation in a swinging Bucket rotor and again spun down to remove excess sodium bromide resulting in white pellets of pPS.

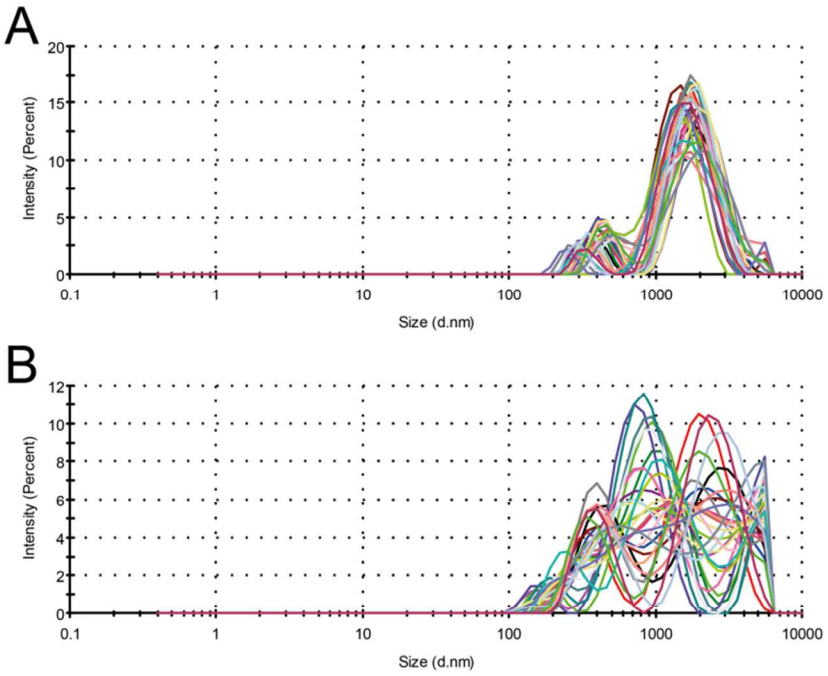

Figure S2: Influence of temperature on pPS fluidity/structure. Size analysis of pPS vesicles (40µg/ml protein in Tris-buffered saline) by dynamic light scattering at 4 °C (A) and 37 °C (B). Each graph shows 30 consecutive measurements of the same sample without intermission.

PS of most mammals has a phase transition temperature between 25 and 41 °C. At lower temperatures (A), the lipids and proteins form a rigid structure with a liposomal character, which remains at a stable size showing two peaks at ~ 400 nm and 2000 nm. To fulfill its physiological function, as a reservoir for the surface tension lowering monolayer at the air-blood barrier, the PS vesicles must be highly flexible. Within the phase transition temperature of PS, such as physiological 37 °C (B), dynamic light scattering shows ever-changing peaks within seconds in a range of 100 – 6000 nm. The PS does not act like stable vesicles, but as a continuously changing membranous system, allowing dynamic interactions of NPs with the PS. For this reasons, the determination of NPs aggregation state in the presence of PS is challenging.

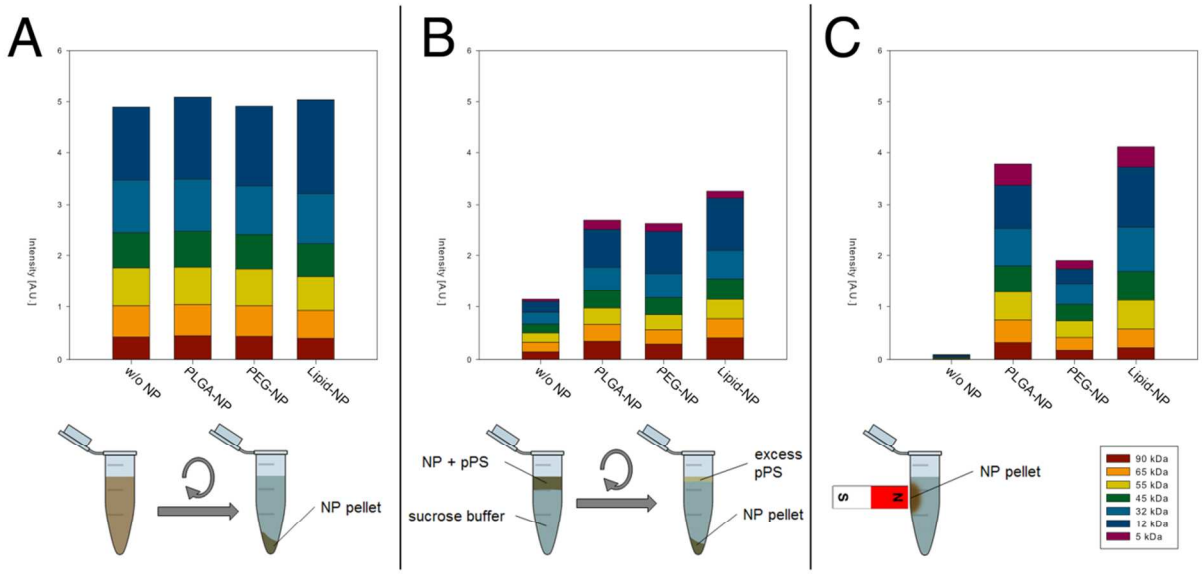

Figure S3: Comparison of different separation methods. Intensities of selected bands after SDS-Page of pPS incubated 1h with PLGA-, PEG-, Lipid-NPs, and w/o NPs, separated by centrifugation (A), density centrifugation (B), and magnetic separation (C).

The high density of the pPS complexes does not allow separation by centrifugation (A). The blank control without NPs showed the same extent of pPS sedimentation as all three NPs. A sucrose cushion of a suitable density also results in the spin down of pPS membranes (B). Density centrifugation demonstrated hardly any difference in the particle corona. Magnetic separation (C) was the only method that resulted in a formation of a negligible pellet in the blank control. Likewise, a presumed distinction between PEG and Lipid particles became obvious and since it was the method with the lowest shear forces and ion strength, it was chosen as superior to the other methods tested.

Table S1: Most abundant lipid species. Top 10 most abundant lipid species found in the corona of PEG-, PLGA-, and Lipid-NPs in comparison to crude pPS as determined by normal phase LC-MS. Values are presented as mean of 3 experiments, each measured three times ±SD.

pPS			**PLGA-NPs**			**PEG-NPs**			**Lipid-NPs**		
Lipid species	**Abundance [%]**		**Lipid species**	**Abundance [%]**		**Lipid species**	**Abundance [%]**		**Lipid species**	**Abundance [%]**	
GPChol(32:0)	36.8	±4.9	GPChol(32:0)	42.5	±2.4	GPChol(32:0)	45.8	±3.1	GPChol(32:0)	44.2	±2.2
GPChol(30:0)	9.0	±2.1	GPChol(30:0)	12.4	±0.8	GPChol(30:0)	12.6	±0.8	GPChol(30:0)	13.3	±0.8
GPChol(34:1)	8.9	±1.2	GPChol(32:1)	11.3	±0.5	GPChol(32:1)	12.0	±1.0	GPChol(34:1)	11.6	±0.6
Cholesterol	7.9	±1.1	GPChol(34:1)	11.1	±0.7	GPChol(34:1)	11.2	±1.0	GPChol(32:1)	11.5	±0.6
GPChol(32:1)	7.0	±0.8	Cholesterol	3.0	±0.5	Cholesterol	1.9	±0.5	Cholesterol	3.1	±0.9
GPIno(34:1)	2.4	±0.3	GPIno(34:1)	2.8	±0.9	GPChol(34:2)	1.6	±0.4	GPIno(34:1)	2.1	±0.5
GPGlyc(34:1)	2.1	±0.4	GPChol(34:2)	1.4	±0.3	GPIno(34:1)	1.5	±0.4	GPChol(34:2)	1.2	±0.2
LGPChol(16:0)	1.6	±0.1	GPChol(34:9)	1.2	±0.3	GPChol(34:9)	1.3	±0.3	GPChol(34:9)	1.0	±0.1
GPGlyc(32:0)	1.1	±0.3	LGPChol(16:0)	1.0	±0.3	GPGlyc(34:1)	0.8	±0.3	GPGlyc(34:1)	0.9	±0.2
GPIno(36:2)	1.0	±0.1	GPGlyc(34:1)	1.0	±0.3	LGPChol(16:0)	0.7	±0.3	LGPChol(16:0)	0.8	±0.2
Top10 Total	**77.7**		**Top10 Total**	**87.8**		**Top10 Total**	**89.4**		**Top10 Total**	**89.6**	

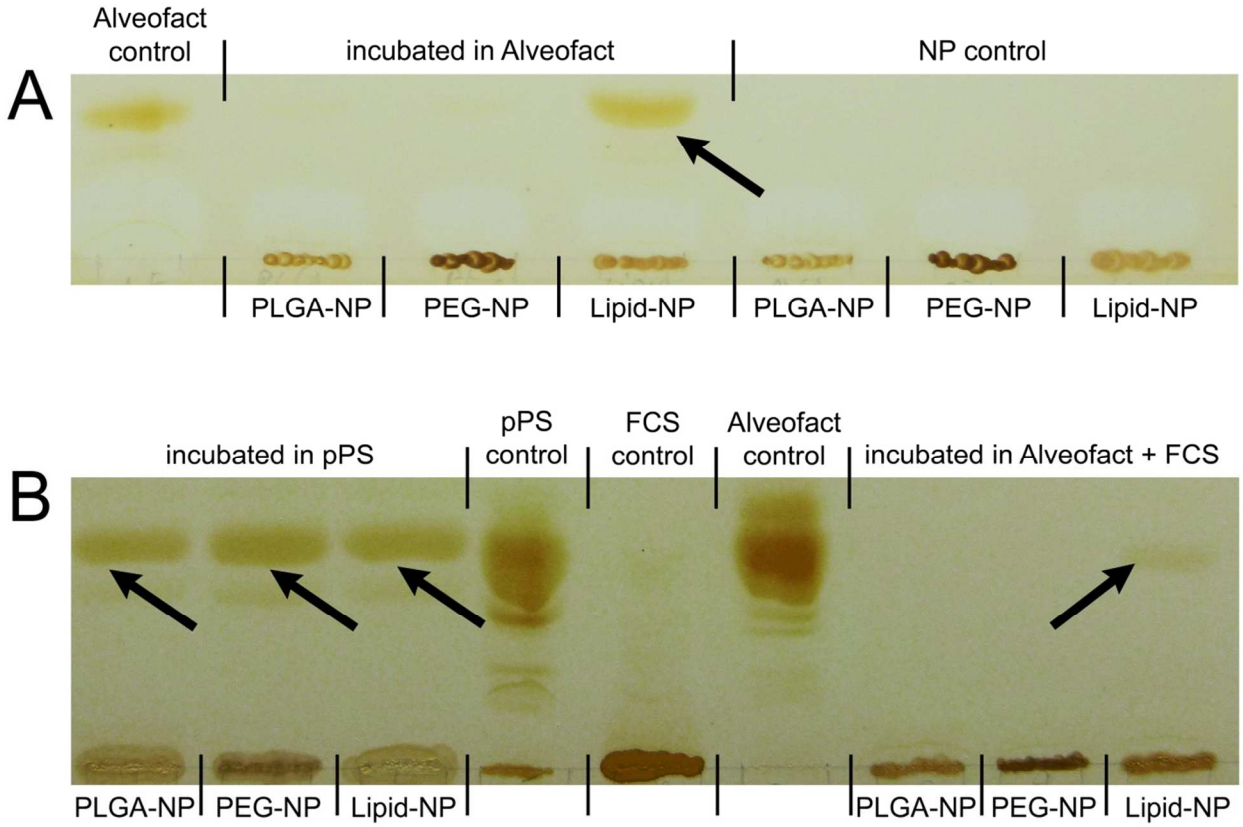

Figure S4: Lipid adsorption on NPs after incubation in Alveofact®, Alveofact® + FCS, and pPS. Thin layer chromatography of PLGA-, PEG-, and Lipid-NPs after 1h incubation at 37°C with the commercially available PS preparation Alveofact® (n=4) (proteins are depleted except for SP-B, and -C) and repeated magnetic separation shows that GPChol (arrow), the most prominent band, has only adsorbed to the Lipid-NPs (A). Alveofact® concentration was chosen to meet the same lipid concentration per µg particles as in pPS (~20 µg phospholipids/µg NPs). Addition of serum proteins (FCS, Lonza, Switzerland) in the same concentration as present in pPS did not change the outcome (right three lanes, n=3). Native pPS with all surfactant proteins shows adsorption of lipids to all used nanoparticles, regardless of their hydrophobicity (left three lines, n=3). The stationary phase was HP-TLC Silica Gel 60, (Merck, Germany), the mobile phase consisted of chloroform:methanol:H_2O 65:25:4. Samples were applied as prepared after incubation and magnetic separation.

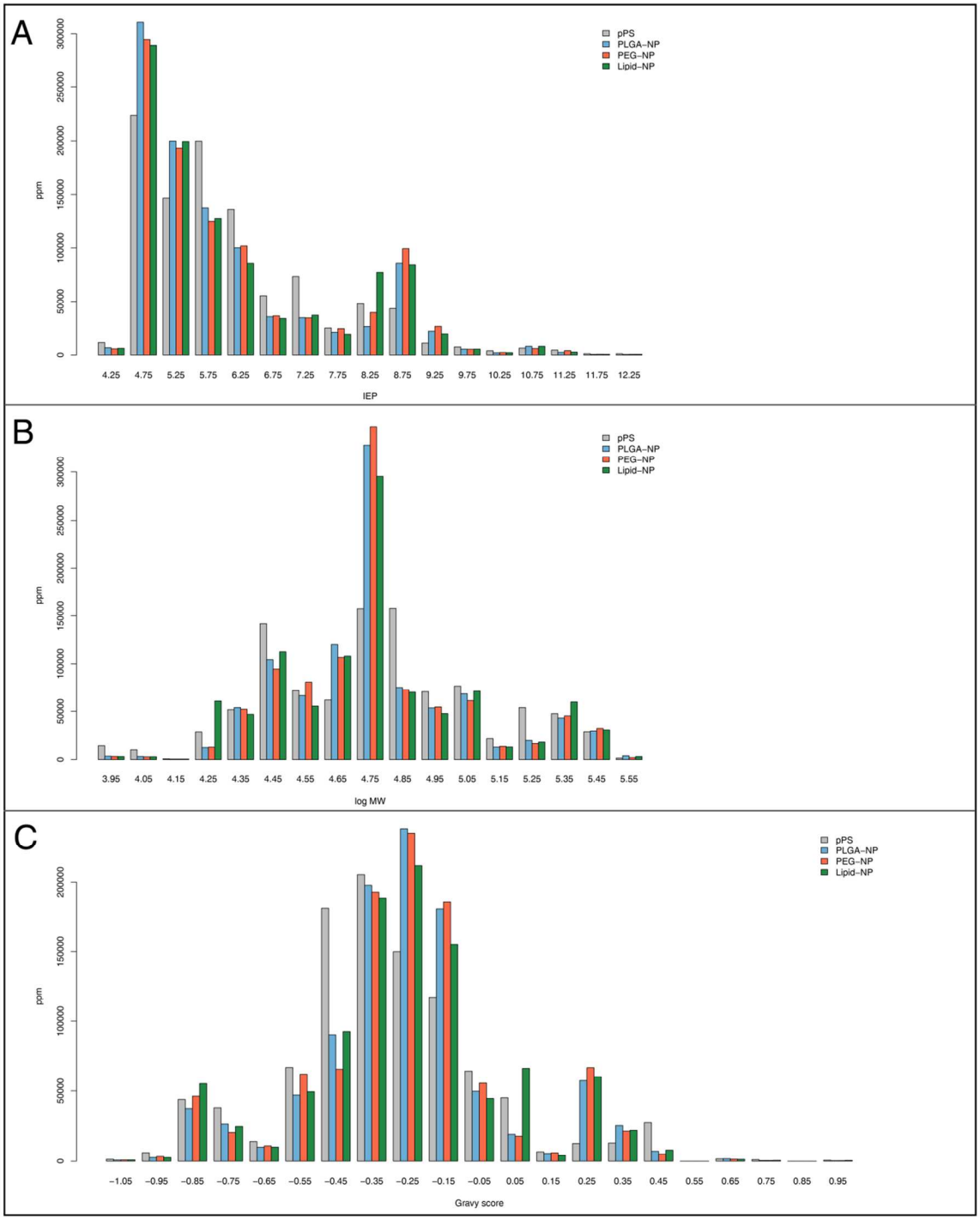

Figure S5 Relative distribution of proteins by their properties. Distribution of found proteins in native surfactant and in the corona of PLGA-, PEG-, and Lipid-NPs in ppm by means of isoelectric point (IEP; A) mol weight (MW; B) and average hydrophobicity (gravy score, C). While the difference between the crude pPS preparation and the NPs is obvious, there is no pattern visible in the adsorbtion behaviour among the nanoparticles. PEG-NPs were expected to attract more hydrophilic proteins, but no such pattern was found.

Table S2: Characterization of nanoparticles

	PLGA-NPs	PEG-NPs	Lipid-NPs
Surface properties	Carboxylic	PEG5000	Phosphatidylcholine
Core	Magnetite/PLGA 50:50	Magnetite/Dextran	Magnetite/GPChol
Source	Synthesis by emulsification-evaporation	Micromod nanomag®-D PEG5000	Chemicell fluidMAG®-Lipid
Size nominal [d.nm]	n.a.	250	200
Z-average (DLS) [d.nm]	217.3 ±3.4	380.0 ±2.1	245.2 ±2.3
PDI (DLS)	<0.1	<0.15	<0.3
Size (NTA) [d.nm]	177 (±47)	160 (±54)	169 (±64)
Zetapotential (DLS) [mV]	-25.1 ±0.3	-13.8 ±0.9	-32.4 ±1.1
Number conc. (NTA) [#/mg]	$8.54*10^{11}$ ($\pm 1.77*10^{11}$)	$7.49*10^{11}$ ($\pm 1.97*10^{11}$)	$4.34*10^{11}$ ($\pm 1.38*10^{11}$)
Calc. surface area [m^2/g]	127	184	82

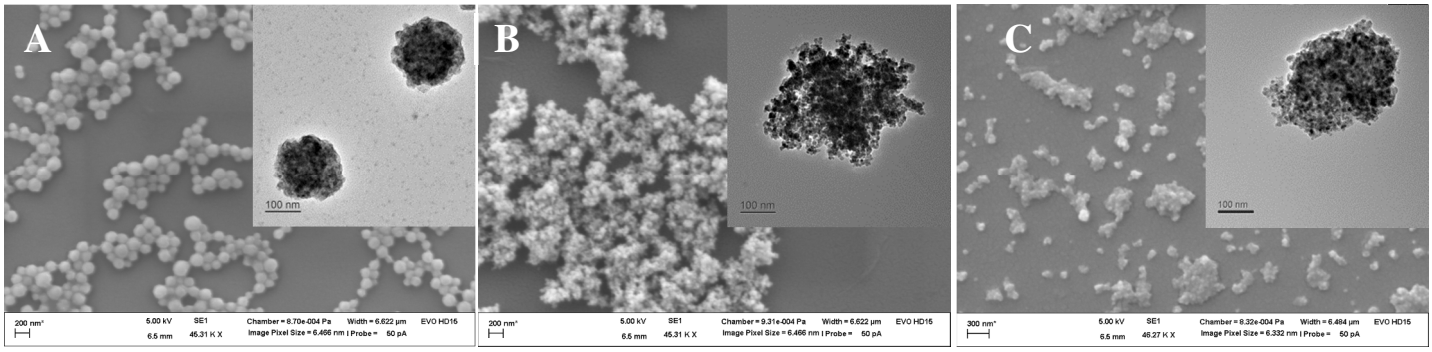

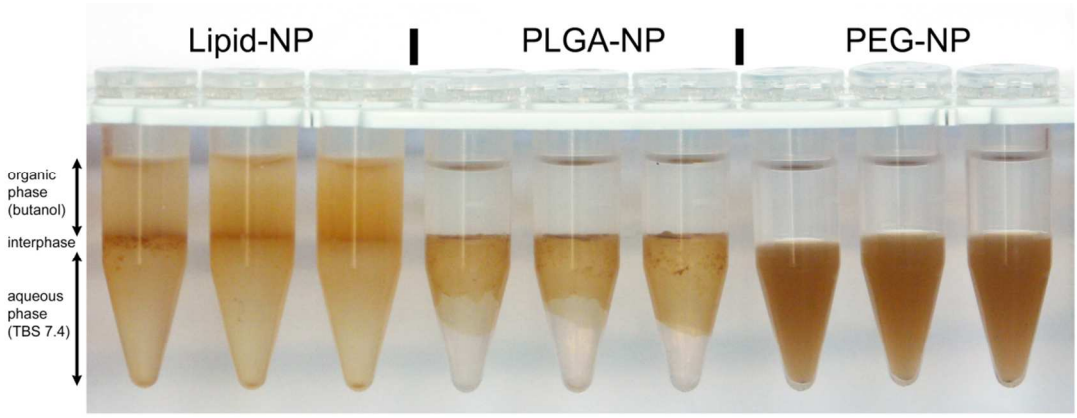

Figure S6 Visual characterization of NPs. A-C**:** SEM (large) and TEM (small – only primary magnetite cores visible) images of magnetic PLGA- (A), PEG- (B) and Lipid-NPs (C). The self-prepared PLGA-NPs are spherical and highly monodisperse, the commercially available PEG- and Lipid-NPs, have a cluster-like shape and show more polydispersity. D shows the distribution of NPs after 24 h equilibration in a saturated mixture of butanol:TBS (pH 7.4) after phase separation. PEG-NPs show no tendency towards the butanol phase whatsoever, while Lipid-NPs are distributed in butanol and aqueous phase with a broad emulsified interphase. PLGA-NPs show a high affinity towards the interphase. With longer standing time, PLGA-NPs crawl down the tube wall but do not disperse in the aqueous phase freely.